20th International Conference on Renewable Energies and Power Quality (ICREPQ'22)
Vigo (Spain), 27th to 29th July 2022
Renewable Energy and Power Quality Journal (RE&PQJ)
ISSN 2172-038 X, Volume No.20, September 2022

Performance of a protection system for DC grids

M.J. Pérez-Molina, P. Eguia, D.M. Larruskain, I. Aranzabal and E. Torres

[1] Department of Electrical Engineering, University of the Basque Country UPV/EHU
Plaza Ingeniero Torres Quevedo, 1, 48013 Bilbao (Spain)
Phone/Fax number: +0034 946 017278, e-mail: **mariajose.perez@ehu.eus**

Abstract. The development of High Voltage Direct Current (HVDC) transmission technology is still challenging due to unresolved technical issues, mostly in terms of protecting the system. The overcurrents and voltage drop produced by fault conditions are severely dangerous to the Voltage Source Converters' (VSC) electronic components. Hence, fast protection systems are needed. This paper proposes a full-selective protection system in conjunction with hybrid HVDC circuit breakers. This protection system employs the rate-of-change-of-voltage and the differential-current algorithms for primary and backup fault protections. This protection scheme is applied to a HVDC grid and an analysis of its performance is presented. This system is evaluated with several fault scenarios that include different fault characteristics. The rate-of-change-of-voltage algorithm's fast operation and the differential-current algorithm's high selectivity are verified.

Key words. VSC-HVDC, Protection system, ROCOV, Differential-current.

1. Introduction

High Voltage Direct Current (HVDC) transmissions are becoming a promising alternative for new expansions of power systems [1]. The development of Voltage Source Converters (VSC) makes possible the prospect of building Multi-Terminal (MT) HVDC grids in the near future.

However, under direct current (DC) fault conditions the voltage collapses sharply and the current rises quickly to very high levels because of the small line resistance. The fault traveling wave propagates rapidly throughout the entire system affecting its components. The fault effects are more problematic on the power electronic devices of the VSCs. Insulated Gate Bipolar Transistors (IGBT) can only withstand twice their nominal current and not the high fault-induced overcurrents [2]. Then, fault conditions have to be detected and cleared in the time range of 10 milliseconds [3], to avoid the damages on the converters [4]. Consequently, fast and reliable detection algorithms have to be developed [5].

In addition, the protection system of Point-to-Point (P2P) HVDC links traditionally uses alternating current (AC) Circuit Breakers (CB) and consequently the system is completely shut down under fault conditions. This kind of fault clearing strategy is not suitable for MT HVDC systems, which makes the evolution from P2P to MT systems challenging [6].

Hence, a more appropriate protection strategy is to use HVDC CBs to isolate only the faulty part of the MT system [7]. Consequently, HVDC CBs have to operate with fast speed, be able to interrupt high currents [8] and to dissipate the energy stored in the system [9].

In order to do this, protection algorithms have to present a selective, fast and accurate operation. A basic classification would be between local-measurement-based algorithms and communication-based algorithms.

Those using only locally available measurements are the so-called local-measurement-based algorithm. They present faster operation speed since they only work with single-ended data but they lack selectivity [10], which can be improved with inductive reactors, delimiting the borders of the protection zone. Furthermore, inductors can limit the rate of rise of the DC current. This way, HVDC CBs must interrupt lower currents but they will have to dissipate a greater amount of energy [11]. Besides, the performance of this type of algorithm is determined by the fault discrimination threshold. The threshold value is selected according to the characteristics of the grid and through simulations. It affects the sensitivity and selectivity of the protection algorithm. A higher value increases the selectivity at the expense of the sensitivity. Local-measurement-based algorithms use directly the current and voltage magnitudes or mathematically process them. Some examples of the first category are the overcurrent [12] and undervoltage [13] algorithms; while among the last category we can find the rate-of-change-of-voltage [14] and rate-of-change-of-current algorithms [15].

Meanwhile, communication-based algorithms use a communication channel to trade information between the borders of the protection zone. The present an inherent selectivity [16] while their operation speed is slower since it depends on the communication time delay [17] and the operation speed requirement might not be satisfied [3] . Consequently, most restrictive parameter in the operation time of a communication-based algorithm is the communication time delay [18]. Moreover, the protection system will be non-operative in the case of a problem in the communication channel [19]. Hence, this type of algorithm is more appropriate for short transmission distances [20], as a backup protection system [21] and for the detection of high impedance fault conditions where the operation speed requirement is not critical to the same degree [22]. The following communication-based algorithms can be mentioned as representative: the directional current [23], which compares the current direction at both ends of the protection zone; and the differential-current algorithm [24], which makes a comparison of the current circulating in and out of the protection zone.

This paper proposes a protection system for HVDC grids. In consequence, the main characteristics of the protection system are detailed in Section 2. The employed hybrid HVDC circuit breakers are detailed in Section II-A as well as the fault clearing strategy (Section 2-B). The protection system combines local-measurement-based and communication-based algorithms for the primary and backup protection of HVDC grids. The selected algorithms are the rate-of-change-of-voltage method (Section 2-C-1) and the differential-current method (Section 2-C-2), respectively. Their combined performance has not been analysed in the literature, to the best of the authors' knowledge. This novel combination allows a more selective and sensitive performance thanks to the combined advantages of both algorithms: the rate-of-change-of-voltage algorithm's fast operation and the differential-current algorithm's high selectivity and reliable operation against high resistance fault conditions. This protection system includes primary and backup protections, adopting a full-selective fault clearing strategy. A faster primary protection is applied while the backup protection allows a highly selective and accurate performance after failure of the primary protection. A study case is presented in Section 3 applying this protection method to a four-terminal symmetric monopole grid. Its performance is analysed against different fault characteristics. Finally, Section 4 presents the conclusions of this work.

2. Proposed protection systems for HVDC grids

Protection systems must avoid damages on components and ensure a continuous and safe system operation during fault conditions and after fault clearance. Consequently, fault isolation and clearance have to be accomplished in the shortest time possible [4], minimizing its impact on the system [25]. Hence, the performance of a protection system has to comply with the requirements of reliability, selectivity, sensitivity, speed and recoverability [26]. Satisfying these requirements is essential to enable a stable and safe operation of the system. The different components of a protection system could affect this stability if they are not adequately selected. Circuit breakers stand out as the main devices considering that they isolate the affected part of the system, interrupt the current and absorb the energy stored in the system. Besides, the adopted fault clearing strategy is a major concern given that it can minimize a fault condition's impact on the system.

The proposed protection system considers primary and backup protections, which are based on different algorithms with parallel operation for the purpose of saving time between the operation of the primary and backup protection systems. The objective is to sum up the benefits of each algorithm and to improve the reliability of the protection system.

A. *Circuit breakers*

HVDC CBs present a fast operation and delimit the system in independent protection zones. Thus, fault isolation is fulfilled without affecting the unaffected parts of the grid, which can continue operating. Accordingly, hybrid CBs are considered for the proposed system. Hybrid HVDC CBs present relatively low on-state losses and fast operation (2-5 ms) [27]. They consist of a main conduction branch with a semiconductor-based load communication switch (LCS) and a fast mechanical switch (FMS), as it is depicted in Fig. 1. The commutation branch's components vary depending on the model, e.g., capacitor snubber circuits [28] or a power electronic breaker [29]. The current circulates through the main conduction branch under normal conditions. When a fault occurs, the LCS commutates the current from the main branch to the commutation branch in order to enable the FMS opening. Finally, the main breaker commutates the current to the energy absorption branch, where surge arresters absorb the energy stored in the system driving the line current to zero.

Besides, limiting inductors can limit the rate of rise of the fault current between the range of the interrupting capability of the HVDC CBs. Moreover, these inductors delimit the protection zone and improve the algorithm's selectivity. Nevertheless, a larger inductor size of requires CBs with a higher energy dissipation capability and might also affect the stability of the system [29].

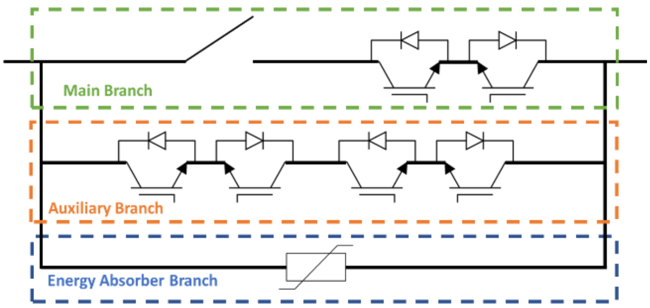

Fig. 1. Scheme of a hybrid HVDC circuit breaker.

B. *Fault Clearing Strategy*

A fault condition's impact on the HVDC and AC grids should be minimized and therefore, the isolated zone of the system should be as small as possible. This way, the damage and stress on the components can be avoided.

Moreover, a shutdown of a large part of the HVDC system can have a relevant impact on the stability of the AC grid.

The selected fault clearing strategy modifies the fault condition's effects on the grid during the fault clearing process [9]. A full-selective fault clearing strategy resembles the traditional AC strategy. Several independent protection zones are demarcated and hybrid HVDC CBs are placed at the limits of each zone. This way, only the faulty zone is disconnected and the healthy zones remain operative. Hence, the fault condition impact is minimized.

C. Proposed protection algorithms

As it has been previously emphasized, the most restrictive requirement for a protection system in HVDC grids is the speed, since fault conditions must be cleared in just a few milliseconds. Due to this, a local-measurement-based algorithm is selected to operate as the main protection in this paper. This main protection algorithm is the rate-of-change-of-voltage (ROCOV) algorithm, which consist of calculating the DC voltage derivative. A communication-based algorithm is also implemented as a backup protection to perform in case of failure in the operation of the primary protection. This backup protection algorithm is a differential-current algorithm. Fibre optic is assumed as the communication channel medium. In addition, the differential-current algorithm is also applied to the high resistance fault protection since these conditions are challenging for the ROCOV operation. Both algorithms work in parallel in order to save time between their operations.

1) Main protection algorithm

The ROCOV algorithm is used as the main protection in this paper. This ROCOV algorithm is selected since a fast operation is one of the essential requirements for a primary protection. The ROCOV algorithm is classified as a local-measurement-based protection method. It employs DC voltage measurements to calculate its derivative as in (1); where V_1 is the voltage magnitude at time t_1 and V_2 is the voltage magnitude at time t_2, being time t_2 greater than time t_1.

$$\mathrm{ROCOV}=\frac{\Delta V}{\Delta t}=\frac{V_2-V_1}{t_2-t_1} \tag{1}$$

Theoretically, the DC voltage is constant during normal operation conditions; therefore, its derivative is zero. Conversely, the DC voltage derivative value increases quickly as the DC voltage drops sharply and almost instantaneously during fault conditions [30]. This characteristic of the ROCOV value makes it a good fault marker [3]. However, the DC voltage is not constant due to fluctuations and disturbances during normal operation conditions in actual systems. Therefore, the fault discrimination is achieved by comparing the DC voltage derivative to a previously selected threshold [17], as in (2).

$$\mathrm{ROCOV}>\mathrm{ROCOV}_{th} \tag{2}$$

The value of the threshold, ROCOVth, depends on the characteristics of the grid and it is selected through simulations [31]. A higher threshold value improves the selectivity at the expense of its sensitivity [32].

2) Backup protection algorithm

The differential-current algorithm is employed as a backup protection in case the main protection operation fails in the proposed protection system.

The differential-current algorithm is a communication-based protection. It is based on summing the input and output currents of a protection zone [3].The input and output currents are equal during normal operation conditions; hence, the differential-current is zero. However, the differential-current value increases quickly during fault conditions since the input and output currents are different. This feature is used as a fault marker. The differential-current on a link Lij is calculated in (3),

$$\mathrm{DiffCurr}_{line}=I_{ij}+I_{ji} \tag{3}$$

where Iij is the current measured at one end of the link and Iji is the current measured at the other end of the link. The reference current direction is shown in Fig. 2.

Fluctuations, disturbances and losses can make the input and output current differ during normal operation conditions. As a result, the differential-current value is compared to a threshold value to allow fault discrimination as in (4) [4].

$$\mathrm{DiffCurr}<\mathrm{DiffCurr}_{th} \tag{4}$$

This method is robust and inherently selective [16]. It also provides directionality [19]. However, it depends on the communication channel and it is limited by the communication speed [2]. In this paper, a communication time delay of 1 ms per 200 km is assumed [33].

3. Study case

This section is focused on the analysis and validation of the combined performance of local-measurement-based and communication-based algorithms for primary and backup protections of a HVDC grid. Several fault conditions are simulated in PSCAD varying parameters as fault distance and fault resistance.

The four-terminal HVDC system shown in Fig. 2 is used in this study case to evaluate the performance of the protection system on PSCAD software [13]. There are five cables interconnecting two onshore AC grids and two offshore wind power plants. Half-bridge modular multilevel converters (MMC) are employed and a symmetric monopole configuration is used. MMC-4 is rated 1200 MVA while the remaining three converters are rated 900 MVA.

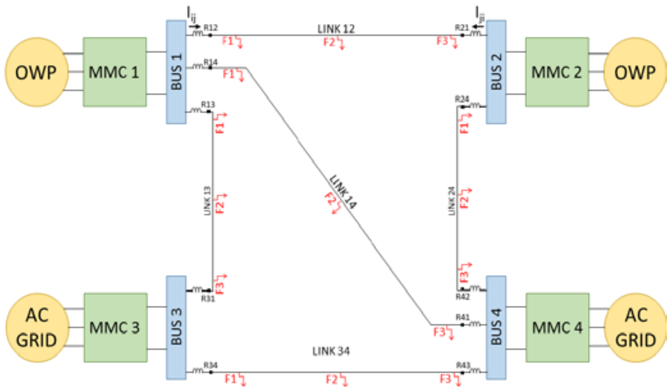

Fig. 2. Single-line diagram of the MT HVDC grid.

The protection philosophy is a full-selective strategy. Hybrid HVDC circuit breakers are placed at both ends of every cable in series with 0.1 H inductive reactors to delimit the protection zone borders. The operation time of the hybrid CB is assumed to be 2 ms. This way, the grid is partitioned in five protection zones, one per link. Cable lengths are 200 km (links 13 and 14), 150 km (link 24) and 100 km (links 12 and 34). As it has been detailed in the previous section, primary protection is a local-measurement-based algorithm, which uses ROCOV for fault detection with a selective threshold of 460,000 kV/ms. Backup protection is a communication-based algorithm based on differential-current. The differential-current protection employs a threshold of 1.5 kA for selectivity purposes. The ROCOV and the differential-current threshold values are selected through simulations [31], identifying the critical values and adding a safety factor to ensure the operation exclusively under internal fault conditions [34]. In this study case, a safety factor of 2 was selected and a sampling rate of 10 kHz was employed.

Several pole-to-pole (PtP) and pole-to-ground (PtG) fault conditions are simulated. Their locations in the links and their resistances are varied. Besides, fault condition F1 is located at the beginning of the link, F2 is located at a distance equal to half of the link length and F3 is located at the end of the link at a distance equal to the link length.

Moreover, these values of fault locations and fault resistances are selected since they are the worst operation conditions in order to check the successful operation of the protection system. The most challenging cases for fault detection are those with the highest fault resistance and where the fault conditions are located at the farthest end of the protection zone from the relay point. From the perspective of current interruption, the worst cases are solid fault conditions located right in front of the relay point. The operation of the protection system is successful for every single simulated case. Thus, only the affected link is isolated while all external relays avoid misdetection and nuisance operation.

A. Low resistance fault condition analysis

Both protection algorithms are firstly analysed for different 0.01 Ω fault conditions changing the affected link and the fault distance. Table I summarises the analysis' results, where the detection time (tdet) is the time required by the corresponding algorithm to detect the fault condition. The maximum current (Imax) is the maximum current magnitude handled by the HVDC CB during its operation. The difference between the detection times of both algorithms (Δt) represents the time needed by the differential-current-based backup protection to operate after the failure of the ROCOV-based primary protection. The last column shows the nuisance operation of the external relays (NT: not tripping, T: tripping).

The ROCOV-bases primary protection shows a detection time of about 1 ms for the most remote fault conditions (close to 200 km) and tens of microseconds for fault conditions located right in front of the relay point.

Meanwhile, the detection time of the differential-current algorithm is slower. It takes around 1-1.5 ms to detect faults since it depends on the communication time delay, which is higher for longer cable lengths. Consequently, the CBs have to interrupt higher currents when the differential-current protection operates.

On the other hand, the time saved due to the parallel operation of both algorithms is up to 0.5 ms for remote faults while it is up to tens of microseconds for near fault conditions due to the very fast operation of the ROCOV algorithm in those cases.

In addition, Table I shows how no external relay presented a nuisance operation in any of the simulated cases.

B. High resistance fault condition analysis

Hereafter, the same fault conditions are simulated but with higher fault resistances, higher than 200 Ω for PtG faults and higher than 400 Ω for PtP faults. The ROCOV algorithms presents a successful operation for fault resistance values lower than those previously pointed out. However, higher fault resistances make ROCOV-based fault detection very challenging.

The results of the ROCOV-based primary protection and the differential-current-based backup protection are summarised in Table II. Symbols "O" and "X" represent successful and unsuccessful fault detection, respectively.

Any time the ROCOV-based protection fails detecting a simulated fault case, the differential-current-based protection successfully detects it. This way, the reliability and sensitivity of the combined protection system is improved. Once again, no nuisance operation of the external relays took place.

On the other hand, the detection time of the differential-current algorithm is affected by the high resistance fault conditions since the differential-current value takes longer to exceed the detection threshold. Nevertheless, the magnitude of the high-resistance-fault-induced currents are lower than in the case of low resistance fault conditions since the rate of increase of the fault current is not as sharp as in low resistance fault conditions.

Table I. - Performance comparison of the ROCOV and the differential-current algorithms for 0.01 Ω fault conditions.

Fault type		R_{AB} ROCOV tdet (ms)	R_{AB} ROCOV Imax (kA)	R_{AB} Diff. Current tdet (ms)	R_{AB} Diff. Current Imax (kA)	R_{AB} Δt (ms)	R_{BA} ROCOV tdet (ms)	R_{BA} ROCOV Imax (kA)	R_{BA} Diff. Current tdet (ms)	R_{BA} Diff. Current Imax (kA)	R_{BA} Δt (ms)	External Relays
Pole to Ground	L12-F1	0.010	4.233	1.060	5.978	1.050	0.560	3.549	1.060	4.478	0.500	NT
	L13-F1	0.010	5.219	1.550	7.514	1.540	1.110	3.293	1.550	3.820	0.440	NT
	L14-F3	1.110	5.356	1.550	5.819	0.440	0.010	3.992	1.550	6.274	1.540	NT
	L24-F1	0.010	4.454	1.320	6.037	1.310	0.830	4.000	1.320	4.116	0.490	NT
	L34-F1	0.010	3.171	1.070	4.829	1.060	0.560	4.644	1.070	5.325	0.510	NT
Pole to Pole	L12-F1	0.010	4.814	1.050	7.272	1.040	0.560	4.915	1.050	5.239	0.490	NT
	L13-F1	0.010	5.807	1.540	8.435	1.530	1.110	4.585	1.540	4.933	0.430	NT
	L14-F3	1.110	5.928	1.540	6.408	0.430	0.010	4.634	1.540	8.004	1.530	NT
	L24-F1	0.010	5.737	1.300	6.783	1.290	0.830	4.616	1.300	4.795	0.470	NT
	L34-F1	0.010	4.456	1.060	6.625	1.050	0.560	5.174	1.060	5.828	0.500	NT

Table II. Performance of the combined algorithms for high resistance fault conditions.

Fault type			RAB ROCOV value (kV/ms)	RAB ROCOV trip	RAB Diff. Current value (kA)	RAB Diff. Current trip	RAB tdet (ms)	RAB Imax (kA)	RBA ROCOV value (kV/ms)	RBA ROCOV trip	RBA Diff. Current value (kA)	RBA Diff. Current trip	RBA tdet (ms)	RBA Imax (kA)	External Relays
Pole to Ground	L12-F1	250 Ω	481,930	O	0.043	X	0.590	0.577	399,742	X	1.504	O	2.910	1.190	NT
	L13-F2	200 Ω	367,789	X	1.501	O	3.880	1.874	367,773	X	1.505	O	3.880	0.131	NT
	L14-F3	250 Ω	400,694	X	1.501	O	4.310	1.508	370,664	X	1.500	O	4.310	0.217	NT
	L24-F1	250 Ω	449,300	X	1.506	O	3.740	1.508	399,172	X	1.505	O	3.740	0.247	NT
	L34-F2	200 Ω	440,144	X	1.513	O	2.540	0.536	440,078	X	1.506	O	2.540	1.621	NT
Pole to Pole	L12-F1	450 Ω	498,441	O	0.042	X	0.580	0.688	438,224	X	1.514	O	2.420	1.516	NT
	L13-F2	400 Ω	367,929	X	1.501	O	3.510	1.968	367,899	X	1.506	O	3.510	0.406	NT
	L14-F3	400 Ω	470,543	O	0.023	X	0.010	1.237	449,641	X	1.501	O	6.290	2.066	NT
	L24-F1	450 Ω	474,991	O	0.073	X	0.900	1.620	437,584	X	1.512	O	3.110	1.059	NT
	L34-F2	400 Ω	440,305	X	1.512	O	2.270	0.700	440,223	X	1.515	O	2.270	1.684	NT

4. Conclusions

A full-selective protection system employing hybrid CBs is proposed. The primary protection uses the ROCOV algorithm as a fault marker while the backup protection consists of the differential-current algorithm. Their combined performance is validated in a four-terminal VSC-HVDC grid modelled in PSCAD software against different fault conditions.

The ROCOV algorithm presents a very fast detection time meanwhile the performance of the differential-current-based backup protection is restricted by the communication time delay (1 ms per 200 km). Besides, the circuit breaker will have to perform under lower fault current conditions when the ROCOV algorithms operates compared to the differential-current algorithm's operation.

Moreover, the parallel operation of both algorithms enables the operation of the backup protection after the failure of the primary protection saving around 0.5 ms for remote fault conditions. However, the ROCOV-based protection is not capable of detecting the fault condition when the fault resistance increases (over 200 Ω and 400 Ω for PtG and PtP, respectively) while the differential-current-based protection operates successfully regardless of the fault resistance.

Therefore, this full-selective protection system provides a fast primary protection and an inherently selective backup protection by combining the advantageous characteristics of the ROCOV and the differential-current methods. Therefore, the parallel operation of both algorithms ensures a reliable and sensitive protection which is suitable for HVDC grids even in the case of high resistance faults.

Acknowledgement

The authors gratefully acknowledge the support from the Basque Government (GISEL research group IT1191-19) and the University of the Basque Country UPV/EHU (GISEL research group 181/18 and PIF20/06).

References

[1] CIGRÉ WG B4.52, "HVDC Grid Feasibility Study," Cigré, 2013. Available: https://e-cigre.org/publication/533-hvdc-grid-feasibility-study (accessed on 19 December 2019).

[2] S. Le Blond, R. Bertho, D. V. Coury and J. C. M. Vieira, "Design of protection schemes for multi-terminal HVDC systems," Renewable and Sustainable Energy Reviews, vol. 56, pp. 965-974, 2016. . DOI: //doi.org/10.1016/j.rser.2015.12.025.

[3] R. Li and L. Xu, "Review of DC fault protection for HVDC grids," WIREs Energy and Environment, vol. 7, (2), 2018. . DOI: 10.1002/wene.278.

[4] M. Farhadi and O. A. Mohammed, "Protection of multi-terminal and distributed DC systems: Design challenges and techniques," Electric Power Systems Research, vol. 143, pp. 715-727, 2017. . DOI: //doi.org/10.1016/j.epsr.2016.10.038.

[5] S. Azazi, M. Sanaye-Pasand, M. Abedini and A. Hasani, "A Traveling-Wave-Based Methodology for Wide-Area Fault Location in Multiterminal DC Systems," IEEE Transactions on Power Delivery, vol. 29, (6), pp. 2552-2560, 2014. . DOI: 10.1109/TPWRD.2014.2323356.

[6] Q. Yang, S. Le Blond, R. Aggarwal, Y. Wang and J. Li, "New ANN method for multi-terminal HVDC protection relaying," Electric Power Systems Research, vol. 148, pp. 192–201, 2017. . DOI: 10.1016/j.epsr.2017.03.024.

[7] K. Sano and M. Takasaki, "A Surgeless Solid-State DC Circuit Breaker for Voltage-Source-Converter-Based HVDC Systems," IEEE Transactions on Industry Applications, vol. 50, (4), pp. 2690-2699, 2014. . DOI: 10.1109/TIA.2013.2293819.

[8] J. Descloux, B. Raison and J. Curis, "Protection strategy for undersea MTDC grids," in 2013 IEEE Grenoble Conference, Grenoble, France, 16-20 June 2013, 2013, . DOI: 10.1109/PTC.2013.6652286.

[9] W. Leterme, I. Jahn, P. Ruffing, K. Sharifabadi and D. Van Hertem, "Designing for High-Voltage dc Grid Protection: Fault Clearing Strategies and Protection Algorithms," IEEE Power and Energy Magazine, vol. 17, (3), pp. 73-81, 2019. . DOI: 10.1109/MPE.2019.2897188.

[10] G. Buigues, V. Valverde, I. Zamora, D. M. Larruskain, O. Abarrategui and A. Iturregi, "DC fault detection in VSC-based HVDC grids used for the integration of renewable energies," in 2015 International Conference on Clean Electrical Power (ICCEP), Taormina, Italy, 16-18 June 2015, 2015, pp. 666-673. DOI: 10.1109/ICCEP.2015.7177591.

[11] D. Jovcic, G. Tang and H. Pang, "Adopting Circuit Breakers for High-Voltage dc Networks: Appropriating the Vast Advantages of dc Transmission Grids," IEEE Power and Energy Magazine, vol. 17, (3), pp. 82-93, 2019. . DOI: 10.1109/MPE.2019.2897408.

[12] J. Yang, J. E. Fletcher, J. O'Reilly, G. P. Adam and S. Fan, "Protection scheme design for meshed VSC-HVDC transmission systems of large-scale wind farms," in 9th IET International Conference on AC and DC Power Transmission (ACDC 2010), London, UK, 19-21 October 2010, 2010, . DOI: //doi.org/10.1049/cp.2010.0996.

[13] W. Leterme, N. Ahmed, J. Beerten, L. Ängquist, D. V. Hertem and S. Norrga, "A new HVDC grid test system for HVDC grid dynamics and protection studies in EMT-type software," in 11th IET International Conference on AC and DC Power Transmission, Birmingham, UK, 10-12 February 2015, 2015, . DOI: 10.1049/cp.2015.0068.

[14] J. Sneath and A. D. Rajapakse, "DC fault protection of a nine-terminal MMC HVDC grid," in 11th IET International Conference on AC and DC Power Transmission, Birmingham, UK, 10-12 February 2015, 2015, pp. 1-8. DOI: 10.1049/cp.2015.0082.

[15] N. Geddada, Y. M. Yeap and A. Ukil, "Experimental Validation of Fault Identification in VSC-Based DC Grid System," IEEE Transactions on Industrial Electronics, vol. 65, (6), pp. 4799-4809, 2018. . DOI: 10.1109/TIE.2017.2767560.

[16] A. K. Marten, C. Troitzsch and D. Westermann, "Non-telecommunication based DC line fault detection methodology for meshed HVDC grids," IET Generation, Transmission & Distribution, vol. 10, (16), pp. 4321-4239, 2016. . DOI: 10.1049/cp.2015.0009.

[17] I. Jahn, N. Johannesson and S. Norrga, "Survey of methods for selective DC fault detection in MTDC grids," in 13th IET International Conference on AC and DC Power Transmission (ACDC 2017), Manchester, UK, 14-16 February 2017, 2017, pp. 1-7. DOI: 10.1049/cp.2017.0041.

[18] M. J. Pérez-Molina, D. M. Larruskain, P. Eguia Lopez, O. Abarrategi and M. Santos-Mugica, "A comparison of non-unit and unit protection algorithms for HVDC grids," in AEIT HVDC International Conference 2019, Florence, Italy, 9-10 May 2019, 2019, . DOI: 10.1109/AEIT-HVDC.2019.8740430.

[19] V. Psaras, A. Emhemed, G. Adam and G. M. Burt, "Review and evaluation of the state of the art of DC fault detection for HVDC grids," in 2018 53rd International Universities Power Engineering Conference (UPEC), Glasgow, Scotland, 4-7 September 2018, 2018, . DOI: 10.1109/UPEC.2018.8541961.

[20] I. Dallas and C. Booth, "Teleprotection in multi-terminal HVDC supergrids," in 12th IET International Conference on Developments in Power System Protection (DPSP 2014), Copenhagen, Denmark, 31 March-3 April 2014, 2014, pp. 1-6. DOI: 10.1049/cp.2014.0015.

[21] D. Naidoo and N. M. Ijumba, "HVDC line protection for the proposed future HVDC systems," in 2004 International Conference on Power System Technology. PowerCon 2004, Singapore, Singapore, 21-24 November 2004, 2005, pp. 1327-1332 Vol.2. DOI: 10.1109/ICPST.2004.1460207.

[22] W. Leterme, J. Beerten and D. Van Hertem, "Nonunit Protection of HVDC Grids With Inductive DC Cable Termination," IEEE Transactions on Power Delivery, vol. 31, (2), pp. 820-828, 2016. . DOI: 10.1109/TPWRD.2015.2422145.

[23] E. Kontos, R. T. Pinto, S. Rodrigues and P. Bauer, "Impact of HVDC Transmission System Topology on Multiterminal DC Network Faults," IEEE Transactions on Power Delivery, vol. 30, (2), pp. 844-852, 2015. . DOI: 10.1109/TPWRD.2014.2357056.

[24] A. Adamczyk, C. D. Barker and H. Ha, "Fault detection and branch identification for HVDC grids," in 12th IET International Conference on Developments in Power System Protection (DPSP 2014), Copenhagen, Denmark, 31 March-3 April 2014, 2014, . DOI: 10.1049/cp.2014.0013.

[25] W. Leterme and D. Van Hertem, "Classification of fault clearing strategies for HVDC grids," in CIGRÉ Lund Symposium, Lund, Sweden, 27-28 May 2015, 2015, .

[26] W. Leterme and D. Van Hertem, "DC fault phenomena and DC grid protection," in HVDC Grids : For Offshore and Supergrid of the Future, D. Van Herterm, O. Gomis-Bellmunt and J. Liang, Eds. [Piscataway, NJ]; Hoboken, New Jersey: IEEE Press; Wiley, 2016, pp. 345-370.

[27] C. C. Davidson, R. S. Whitehouse, C. D. Barker, J. Dupraz and W. Grieshaber, "A new ultra-fast HVDC circuit breaker for meshed DC networks," in 11th IET International Conference on AC and DC Power Transmission, Birmingham, UK, 10-12 Feb. 2015, 2015, pp. 1-7. DOI: 10.1049/cp.2015.0021.

[28] C. Meyer, M. Kowal and R. W. De Doncker, "Circuit breaker concepts for future high-power DC-applications," in Fourtieth IAS Annual Meeting. Conference Record of the 2005 Industry Applications Conference, Kowloon, Hong Kong, China, 2-6 October 2005, 2005, pp. 860-866. DOI: 10.1109/IAS.2005.1518439.

[29] J. Häfner and B. Jacobson, "Proactive hybrid HVDC breakers - A key innovation for reliable HVDC grids," in The Electric Power System of the Future - Integrating Supergrids and Microgrids International Symposium, Bologna, Italy, 13-15 September 2011, 2011, .

[30] M. J. Pérez Molina, D. M. Larruskain, P. Eguía López and A. Etxegarai, "Analysis of Local Measurement-Based Algorithms for Fault Detection in a Multi-Terminal HVDC Grid," Energies, vol. 12, (24), 2019. . DOI: 10.3390/en12244808.

[31] B. Li, J. He, Y. Li and B. Li, "A review of the protection for the multi-terminal VSC-HVDC grid," Protection and Control of Modern Power Systems, vol. 4, (1), pp. 21, 2019. . DOI: 10.1186/s41601-019-0136-2.

[32] M. J. Pérez-Molina, D. M. Larruskain, P. Eguía López and G. Buigues, "Challenges for Protection of Future HVDC Grids," Frontiers in Energy Research, vol. 8, 2020. . DOI: 10.3389/fenrg.2020.00033.

[33] J. Descloux, P. Rault, S. Nguefeu, J. Curis, X. Guillaud, F. Colas and B. Raison, "HVDC meshed grid: Control and protection of a multi-terminal HVDC system," in CIGRÉ Session Paris, Paris, France, 26-31 August 2012, 2012, pp. 10.

[34] M. J. Pérez-Molina, P. Eguia, D. M. Larruskain, G. Buigues and E. Torres, "Non-unit ROCOV scheme for protection of multi-terminal HVDC systems," in 22nd European Conference on Power Electronics and Applications (EPE ECCE Europe 2020), Lyon, France, 7-11 September 2020, 2020, . DOI: 10.1109/melecon48756.2020.9140642.